



EDGEWOOD

CHEMICAL BIOLOGICAL CENTER

U.S. ARMY RESEARCH, DEVELOPMENT AND ENGINEERING COMMAND

ECBC-TR-415

CORRELATION OF MASS SPECTROMETRY IDENTIFIED BACTERIAL BIOMARKERS FROM A FIELDED PYROLYSIS-GAS CHROMATOGRAPHY-ION MOBILITY SPECTROMETRY BIODETECTOR WITH THE MICROBIOLOGICAL GRAM STAIN CLASSIFICATION SCHEME

A. Peter Snyder
Waleed M. Maswadeh
Charles H. Wick

RESEARCH AND TECHNOLOGY DIRECTORATE

Jacek P. Dworzanski
Ashish Tripathi



GEO-CENTERS

GEO-CENTERS, INC., GUNPOWDER BRANCH

September 2005

Approved for public release;
distribution is unlimited.



20051212 034

ABERDEEN PROVING GROUND, MD 21010-5424

Disclaimer

The findings in this report are not to be construed as an official Department of the Army position unless so designated by other authorizing documents.

REPORT DOCUMENTATION PAGE

Form Approved
OMB No. 0704-0188

Public reporting burden for this collection of information is estimated to average 1 hour per response, including the time for reviewing instructions, searching existing data sources, gathering and maintaining the data needed, and completing and reviewing this collection of information. Send comments regarding this burden estimate or any other aspect of this collection of information, including suggestions for reducing this burden to Department of Defense, Washington Headquarters Services, Directorate for Information Operations and Reports (0704-0188), 1215 Jefferson Davis Highway, Suite 1204, Arlington, VA 22202-4302. Respondents should be aware that notwithstanding any other provision of law, no person shall be subject to any penalty for failing to comply with a collection of information if it does not display a currently valid OMB control number. **PLEASE DO NOT RETURN YOUR FORM TO THE ABOVE ADDRESS.**

Blank

EXECUTIVE SUMMARY

A pyrolysis-gas chromatography-ion mobility spectrometry (Py-GC-IMS) briefcase system can detect and classify deliberately released bioaerosols in outdoor field scenarios. The bioaerosols include Gram-positive spores and Gram-negative bacteria, the MS-2 *Escherichia coli*ophage virus, and ovalbumin (OV) protein species. However, the origin and structural identities of the pyrolyzate peaks observed in the GC-IMS dataspace, their microbiological information content, and taxonomic importance with respect to biodetection have not been determined.

The present work interrogates the identities of the peaks by inserting a time-of-flight (TOF) mass spectrometry (MS) system in parallel with the IMS detector through a Tee connection in the GC module. Biological substances, producing ion mobility peaks from the pyrolysis of microorganisms, have been identified by their GC retention times, by matching their electron ionization mass spectra with authentic standards, and by the National Institute of Standards and Technology (NIST) mass spectral database.

Strong signals from 2-pyridinecarboxamide were identified in *Bacillus* samples, including *Bacillus anthracis*, and their origins were traced to the cell wall peptidoglycan macromolecule. 3-Hydroxymyristic acid is a component of lipopolysaccharides (LPS) in the cell walls of Gram-negative organisms. The Gram-negative *E. coli* organism showed significant amounts of 3-Hydroxymyristic acid derivatives and degradation products in Py-GC-MS analyses. Some of the fatty acid derivatives were observed in very low abundance in the ion mobility spectra and the highest boiling lipid species were absent.

Improvements that can be applied to the IMS detector are addressed. Biological compounds, predominately found or only found in Gram-positive or Gram-negative bacterial cell walls, contain microbiological taxonomy information and can be considered as biomarkers. Mass spectral analyses of bacterial pyrolyzates have confirmed the presence of biomarker compounds generated from the Py-GC module in the briefcase Py-GC-IMS system. Evidence is presented that the Py-GC-ambient temperature and pressure-IMS system generates and detects bacterial biochemical information that can serve as components of a biological classification scheme directly correlated to the Gram stain reaction in microorganism taxonomy.

Blank

PREFACE

The work described in this report was authorized under Project No. 206023.84BPO. This work was started in October 2002 and completed in December 2003.

The use of either trade or manufacturers' names in this report does not constitute an official endorsement of any commercial products. This report may not be cited for purposes of advertisement.

This report has been approved for public release. Registered users should request additional copies from the Defense Technical Information Center; unregistered users should direct such requests to the National Technical Information Service.

Blank

CONTENTS

1.	INTRODUCTION	9
2.	EXPERIMENTATION.....	11
2.1	Materials.....	11
2.2	Bacteria Preparation	11
2.3	Pyrolysis-Gas Chromatography-Ion Mobility Spectrometry-Mass Spectrometry	12
2.4	Data Analysis	14
3.	RESULTS AND DISCUSSION	15
3.1	Gram-positive Bacterial Spores	15
3.2	Gram-positive Vegetative Cells	18
3.3	Gram-negative <i>E. coli</i>	23
3.4	Biomarker Taxonomic Utility	24
3.5	Improvement of Py-GC-IMS Performance.....	26
3.6	Multivariate Data Analysis	26
4.	CONCLUSIONS.....	27
	LITERATURE CITED	31

FIGURES

1.	Py-GC-IMS-MS System	13
2.	Py-GC-IMS and Py-GC-MS Chromatograms of Gram-positive BG Spores	16
3.	Py-GC-IMS and Py-GC-MS Chromatograms of the Gram-positive Δ Texas Vegetative Strain of <i>B. anthracis</i>	22
4.	Py-GC-IMS and Py-GC-MS Chromatograms of Gram-negative <i>E. coli</i> K-12	25
5.	DF Plots of the Analysis of Liquid Suspensions of Gram-positive, Gram-negative, and Protein Biological Species	28

TABLE

GC-MS Identified Pyrolysis Products	19
---	----

**CORRELATION OF MASS SPECTROMETRY IDENTIFIED BACTERIAL BIOMARKERS
FROM A FIELDED PYROLYSIS-GAS CHROMATOGRAPHY-ION MOBILITY
SPECTROMETRY BIODETECTOR WITH THE MICROBIOLOGICAL GRAM STAIN
CLASSIFICATION SCHEME**

1. INTRODUCTION

Outdoor analytical systems that detect biological and chemical substances usually trace their roots to the configuration and performance standards of their laboratory-based counterparts. Fielded instruments are often compromised in their performance evaluation because of logistics and parameters such as

- Operator portability or transportability,
- Small configuration and footprint,
- Lack of bottled gas,
- Extended times of unattended operation,
- Low maintenance,
- Turnkey start-up,
- Lack of chemical and biological substance expendables, and
- Low power requirements.

Analytical ion mobility spectrometry (IMS) is being used in field and laboratory research and technology applications. The system is straightforward in concept and design.^{1,2} A nickel-63 radioactive ionization source converts sample vapor into ions, which drift through an electric field gradient in a linear tube between a pulsed voltage shutter grid and a Faraday plate ion current detector. When operated in the low Torr regime under laboratory conditions interfaced in series with a time-of-flight mass spectrometry (TOF-MS) system, an IMS detector can obtain a separation of complex mixtures. This procedure has been reported by Hoaglund-Hyzer³⁻⁵ with bacterial proteome extracts, Gillig *et al.*⁶⁻⁹ with lipids and peptides, Matz *et al.*¹⁰⁻¹² on amino acids, peptides and protein conformation, and Lee *et al.*¹³⁻¹⁶ on carbon cluster compounds. However, when an IMS detector is operated at close to atmospheric pressure, lower performance characteristics become evident.¹

Atmospheric pressure IMS is well suited to outdoor, field applications.^{1,2,17-23} Field utility of IMS is attractive because the system is easily portable and has low logistics and consumable requirements. The IMS can be characterized as a TOF-MS detector at atmospheric pressure because the significant resistance between the sample ions and the atmospheric molecules compromises the resolution of the instrument and inherent information potential of the ions.

Pyrolysis (Py) converts a solid sample to vapors by rapid heating and gas chromatography (GC) separates a vapor mixture into its individual constituents. Py-GC is a convenient method for processing solid samples and transferring the resulting fractionated vapor into an atmospheric pressure IMS detector. Therefore, large solid biological substances such as

proteins and bacteria^{17-20, 24} can be interrogated by IMS through their thermal conversion into low mass species.

GC-electron ionization (EI)-MS can provide unambiguous identification of a sample from the GC retention time of a substance and its pattern of masses. GC-MS provides the dimension of time in series with a mass spectrum as the second analytical dimension. GC-IMS, however, consists of two analytical separation stages in series, where the information in both dimensions is time. This situation does not allow for the identification of a compound compared to that of GC-MS.

A laboratory Curie point wire, Py-GC-heated, IMS-MS system was used to investigate the presence of dipicolinic acid (DPA) in microorganisms.²⁵ A Tee was placed in the GC to partition and transfer the biological sample at the same retention time into the ion trap MS and IMS detectors. The presence (Gram-positive organisms) and absence (Gram-negative organisms) of the picolinic acid thermal fragment of DPA in the GC-IMS and GC-MS dataspace were determined. DPA, calcium dipicolinate salt, is found only in Gram-positive bacterial spores (5-15% by weight).^{26, 27}

The Py-GC-IMS laboratory concept^{25, 28} was transformed into a field-operational, briefcase bioaerosol detector, and an aerosol concentrator was interfaced to the pyrolysis source of the system. The IMS detector component is a modified ambient pressure and temperature Chemical Agent Monitor (CAM) that is used by North Atlantic Treaty Organization (NATO) armed forces for the detection and screening of chemical agent vapor.

Outdoor bioaerosols consisting of Gram-positive *Bacillus atrophaeus* ((BG) formerly *Bacillus globigil* var. *niger*), Gram-negative *Pantoea agglomerans* ((EH) formerly *Erwinia herbicola*), ovalbumin protein (OV), and the MS-2 *Escherichia coli*ophage virus were released during formal trials at Western desert and prairie test sites in the United States and Canada.¹⁸⁻²⁰ Differentiation between the four bioaerosols was possible by visual¹⁸⁻²⁰ and multivariate factor analysis determinations²⁹ of the dispersion of pyrolyzate peaks in the GC-IMS dataspace. These tests documented the first successful detection and differentiation of outdoor released bioaerosols with an ambient temperature and pressure IMS detector interfaced to a biological sample Py-GC processing system.

Identification of the biological responses in the GC-IMS dataspace of the briefcase fielded Py-GC-ambient temperature-IMS biodetector is investigated herein by interfacing an EI-TOF-MS system in a parallel configuration similar to that of the Py-GC-IMS-MS laboratory system.²⁵ The analytical mass spectrometer was used to identify the compounds produced and transferred by the Py-GC module in the fielded Py-GC-IMS device. Mass spectral information provided evidence that polar pyrolyzate compounds with significant biological classification information (biomarkers) passed through the torturous Py-GC pathway. However, some of these compounds were spectrally silent in the IMS detector. Heating the IMS cell could enable the observation of more, biologically relevant GC-IMS dataspace peak information in the Py-GC-IMS system.

A biological substance classification and differentiation scheme emerged from the MS-directed identification of the GC-IMS dataspace peaks. The classification scheme consists of two fundamental components: (a) mass spectral identification of pyrolysis generated biochemical species (biomarkers) that are known to be specific to Gram-positive and Gram-negative microorganisms from cell wall and cell surface macromolecular and structural viewpoints, and (b) multivariate discriminant analysis of the specific biomarkers and unidentified peaks in the GC-IMS dataspace. Evidence has been presented that the outdoor fielded Py-GC-ambient temperature and pressure IMS bioaerosol detector produces biochemical information that can be correlated with the Gram stain reaction used for Gram-positive and Gram-negative microorganism taxonomy.

2. EXPERIMENTATION

2.1 Materials.

All protein and biochemical standards were obtained from Sigma-Aldrich (St. Louis, MO) except 2-pyridinecarboxamide, which was purchased from Lancaster Synthesis (Windham, NH) and Staphylococcal Enterotoxin B (SEB), which was purchased from List Biological Laboratories, Inc (Campbell, CA). Peptidoglycan from *Staphylococcus aureus* and lipopolysaccharide (LPS) from *Escherichia coli* K-235, (prepared by phenol extraction) were suspended in methanol (1 mg/mL). Model amino acids, sugars, peptides, proteins and nucleic acids were used as water solutions (1 mg/mL).

2.2 Bacteria Preparation.

Gram-positive vegetative cells of *Bacillus anthracis* (BA) and spores of *B. cereus* ATCC 6464, *B. megaterium*, and BG were prepared as suspensions in deionized, distilled water. The BA strains included VNR1-Δ1, Δ Texas, and Δ Ames. The *bacilli* and suspensions of Gram-negative *Pantoea agglomerans* ATCC 33248 (EH) and *E. coli* K-12 were heat killed. A 1- μ L aliquot of 0.1-5 mg/mL suspensions was used for all bacteria. BG was selected because it produces spore-containing DPA and serves as a surrogate for BA in outdoor aerosol biodetection scenarios. EH was chosen because it does not contain DPA, and it is the only Gram-negative organism approved by the Environmental Protection Agency (EPA) for outdoor, military bioaerosol dissemination studies. Furthermore, EH is used as a surrogate for pathogenic Gram-negative organisms.

For Gram-positive bacterial growth and spore formation, a *Bacillus* culture was streaked for isolation onto an agar plate containing trypticase soy agar (TSA) and 5% sheep's blood. The culture was incubated overnight at 37 °C. A single colony was then streaked onto an agar plate and incubated at 37 °C for about 4-6 hr or until there was visible growth on the plate. The bacterial growth was scraped from the agar plate and suspended in sterile broth or saline. The bacterial suspension (500 μ L) was pipetted onto the surface of nutrient sporulation media in an agar plate and spread evenly with a cell spreader. These plates were incubated at 37 °C for 3 days until spore production reached a maximum. The spore generation was monitored using phase contrast microscopy.

The vegetative cells appeared as dark, oblong cells in short or long chains except for BG which appeared as smaller, highly refractile bodies either within vegetative cells or free-floating. Growth was scraped from the agar plates and washed twice with 200 mL sterile water, resuspended in sterile water, heat-killed, and lyophilized. The vegetative cells were prepared by suspending isolated colonies from TSA and sheep's blood agar plates in sterile water to a density corresponding to a 1-McFarland standard.²⁹ This was diluted 1:10, and 2 mL of the 1:10 suspension was added to 200 mL of nutrient broth. The nutrient broth was incubated overnight at ambient temperature, centrifuged, and washed twice with 200-mL sterile water. The bacterial pellet was resuspended in sterile water, heat-killed, and lyophilized. All the cultures were autoclaved for 20 min to kill vegetative cells and spores. BA preparations were cultured and killed in Biosafety Level (BL) 3 facilities. All other organisms were handled and processed under minimal safety level BL-1 conditions.

For the Gram-negative vegetative organisms, *E. coli* was streaked onto Nutrient Agar plates and EH was grown in *Brucella* broth. Both organisms were incubated for 24 hr at 37 °C. Nutrient broth (10 mL) was placed in a 15-mL conical tube and seeded with the Gram-negative bacteria. The tube was incubated at 37 °C for 24 hr. Nutrient broth (250 mL) was then placed in a 500-mL Erlenmeyer flask and seeded with a 1:10 dilution of a 1-McFarland preparation from the bacterial growth in the 15-mL conical tube. The flask was placed in a shaking incubator at ambient temperature. Aliquots of bacteria in broth were centrifuged at 10,000 rpm for 25 min and washed twice with 200 mL of sterile water. The pellet was resuspended and the aliquots were placed in the pyrolysis module.

2.3

Pyrolysis-Gas Chromatography-Ion Mobility Spectrometry-Mass Spectrometry.

The pyrolysis sample processor consisted of a Pyrex tube (4 mm ID, 8 mm OD, and 5 cm length) with a quartz microfiber filter (type QM-A, thickness 0.45 mm, from Whatman, Hillsboro, OR) supported by a Pyrex frit inside the tube (Figure 1). The Pyrex tube was wrapped with a resistive heater filament (Omega Engineering, Stamford, CT). The heating apparatus was used in two modes of operation: (a) a 10-s mode with the maximum temperature in the tube at 120 °C for drying the moisture and other low boiling volatiles after a sample was deposited on the filter, and (b) a subsequent pyrolysis mode with a maximum temperature of 400 °C in 7 s.¹⁸⁻²⁰

Samples were deposited as water suspensions on the quartz filter. The resulting pyrolysis products were transferred through a heated Silcosteel™ tube, and the injection valve transferred a portion of the sample into the GC column (stainless steel, 4 m x 0.50 mm ID Ultra Alloy) coated with 0.10- μm layer of poly (dimethylsiloxane) from Quadrex (New Haven, CT, USA). The GC was kept in an isothermal mode at 40 °C prior to the pyrolysis event. Ten seconds after pyrolysis, the GC was ramped from 40-140 °C at the rate of 120 °C/min. The temperatures of the pyrolyzer, 3-way injection valve, and GC column were monitored by using type K thermocouples connected to in-house constructed control electronic boards interfaced to a laptop computer.

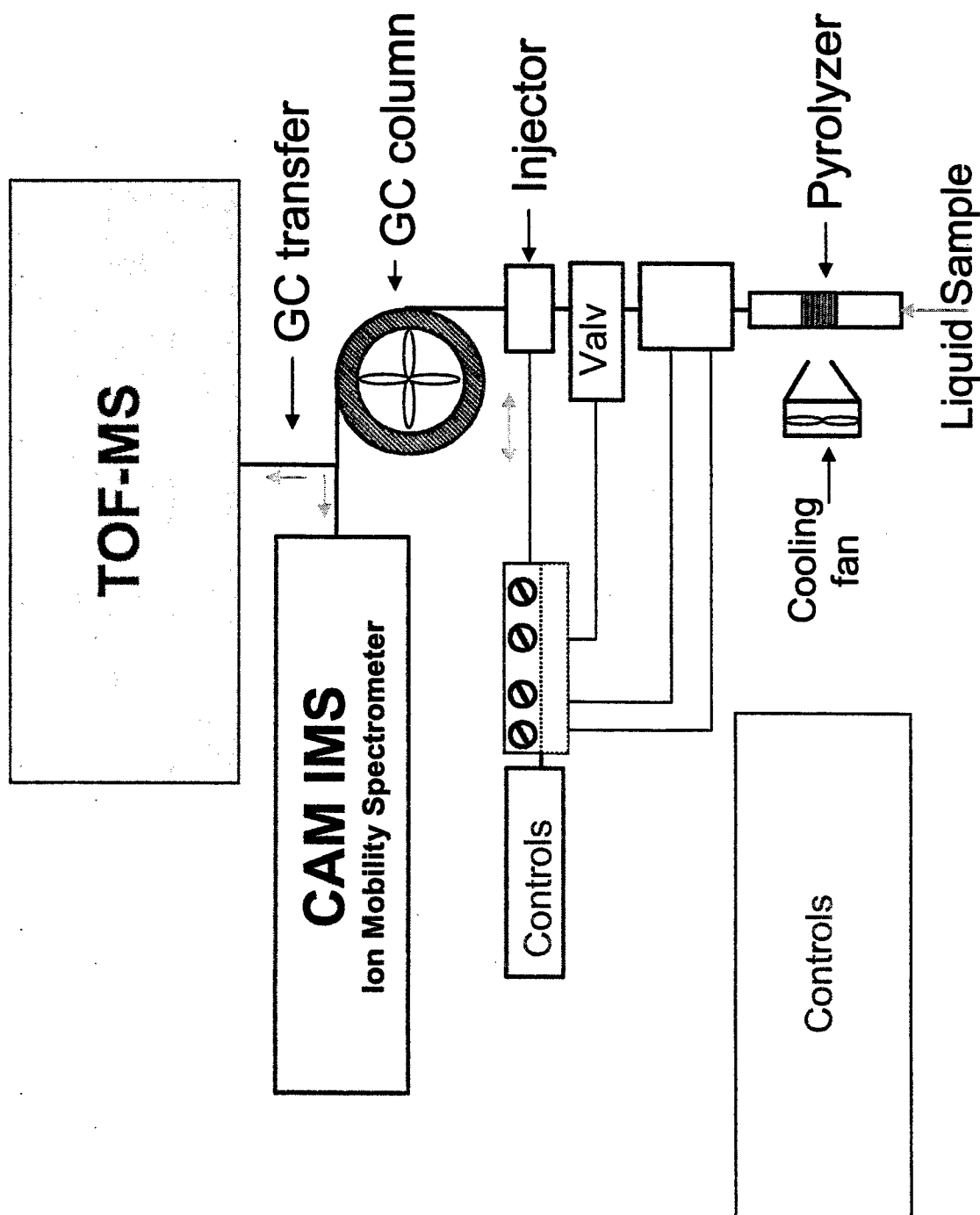


Figure 1. Py-GC-IMS-MS System

The pyrolyzer was kept at atmospheric pressure with nitrogen gas, and the pyrolyzate was transferred into the GC column during a pyrolysis event using a 3-way valve. The exit of the temperature programmable GC column was inserted into a Tee to split the carrier gas between an EI-TOF-MS system (TEMPUS, ThermoFinnigan, San Jose, CA,) and a CAM IMS detector (General Dynamics, DeLand, FL) (Figure 1). The resulting pressure difference between the IMS and MS pumps was used as a driving force for the carrier gas flow during the pyrolyzate transfer and injection steps into and through the GC column. Further details of the Py-GC-IMS system configuration and parameters have been reported elsewhere.²⁰ Alternatively, pyrolysis was conducted under ambient atmospheric air conditions, and the pyrolyzate was captured at the entrance of the GC column at 40 °C. The carrier gas was then changed to nitrogen. The pyrolyzate portion that entered the IMS cell was diluted with an additional nitrogen gas supply to prevent saturation of the Faraday detector. The mass spectral and ion mobility chromatograms produced equivalent GC-MS and GC-IMS information regardless of whether a sample was pyrolyzed under air or nitrogen carrier gas conditions.

The flows of nitrogen gas to the MS and IMS detectors were 3 and 15 mL/min, respectively. These flow rates were determined by the transfer line ID, temperature, and pressure difference between the Tee and each detector. The carrier gas flow rates and both transfer line ID and length dimensions were adjusted so that the GC eluate entered both detectors at the same time.

2.4 Data Analysis.

Multivariate data analysis was applied to the GC-IMS dataspace information from biological substance solutions and suspensions. However, GC-IMS produces a 3-dimensional dataset (3-D) that includes ion drift time, GC retention time, and intensity. Multivariate data analysis can only interrogate 2-dimensional (2-D) information; therefore, the GC-IMS dataspace was converted from 3-D to 2-D data.^{30,31}

An automated peak search was performed on a raw GC-IMS dataspace where the search was conducted at longer drift times than the protonated, water reactant ion peak (RIP) (1). A cell grid (7x14) was placed over the GC-IMS dataspace domain where 14-successive cells were positioned between 5.2- and 11-ms drift times at 0.41-ms intervals on the abscissa. Seven cells were partitioned between 5 and 50 s after pyrolysis in the GC retention time ordinate at 6.4-s intervals, which yielded 98 cells. All the peak intensities in each cell were summed to produce one intensity value per cell. Therefore, one GC-IMS dataspace from the analysis of a sample is represented by a row of $7 \times 14 = 98$ summed intensity values. The 98 cells are transformed into vectors or dimensions in multivariate dataspace that are mathematically orthogonal to each other. The summed intensity value for each cell represents the magnitude for its respective vector or dimension axis.

The first 9-principal component (PC) factors described 95% of the dataset variance. They were used as the variables for discriminant function (DF) analysis of the biological substances. The PC factors were used as variables because the very low cases (experiments) to dimension ratio yielded poor standard deviation statistics.³² The number of cases (experimental replicates) was 20 for each of the 12-different biological substances or

categories (*vide infra*). An additional 24 cases for the “blank” category, consisted of 2 experiments for each of the 12-sample categories. The amount of sample deposited in the pyrolysis region was below the IMS detection threshold of $< 0.05 \mu\text{g}/\mu\text{L}$ and the number of dimensions was 98. The case/dimension ratio = $264/98 = 2.7$, and only 3 cases per dimension yielded poor standard deviation statistics. Instead of a significantly increased number of experimental cases, a reduced number of variables representing the first 9 PC factors was chosen.

3. RESULTS AND DISCUSSION

The use of Py-GC-IMS to detect and provide bacterial aerosol differentiation in outdoor environments has already been published.¹⁷⁻²⁰ However, fundamental performance concerns, such as the microbiological meaning of the various peaks in the GC-IMS dataspace, still remain. Additional concerns are the degree of biochemical analyte throughput in the processing and transfer modules, and the ability of the IMS detector to respond to the GC eluate components.

The Py-GC- ambient temperature and pressure IMS system has been shown to distinguish between BG Gram-positive spores, EH Gram-negative bacteria, and OV protein bioaerosols in outdoor field scenarios.²⁰ This work presents clarification and proof that the Py-GC module of the Py-GC-IMS system provides biochemical information that has microbiological taxonomic meaning from the analysis of bacterial pyrolyzates.

3.1 Gram-positive Bacterial Spores.

Dworzanski, *et al.*³³ have described the performance of the Py-GC module, in the briefcase Py-GC-IMS biodetector, interfaced with a TOF-MS detector in the analyses of biochemicals and microorganisms. Nonspecific and bacteria specific biomarker compounds were observed for Gram-positive bacteria. In addition, plausible pyrolysis decomposition mechanisms for peptidoglycan macromolecule standards and model biochemical compounds were postulated to identify the pyrolysis products and deduce their bacterial origin.

Figure 2 presents data showing the GC-MS total ion chromatogram (TIC) and corresponding peaks in the GC-IMS dataspace for a BG spore sample. Direct correlations are observed between the dominant GC and IMS peaks, which are highlighted by arrows. All major and minor GC peaks have discernible matching peaks in the IMS chromatograms. Therefore, a high degree of visual correlation exists between the two chromatograms.

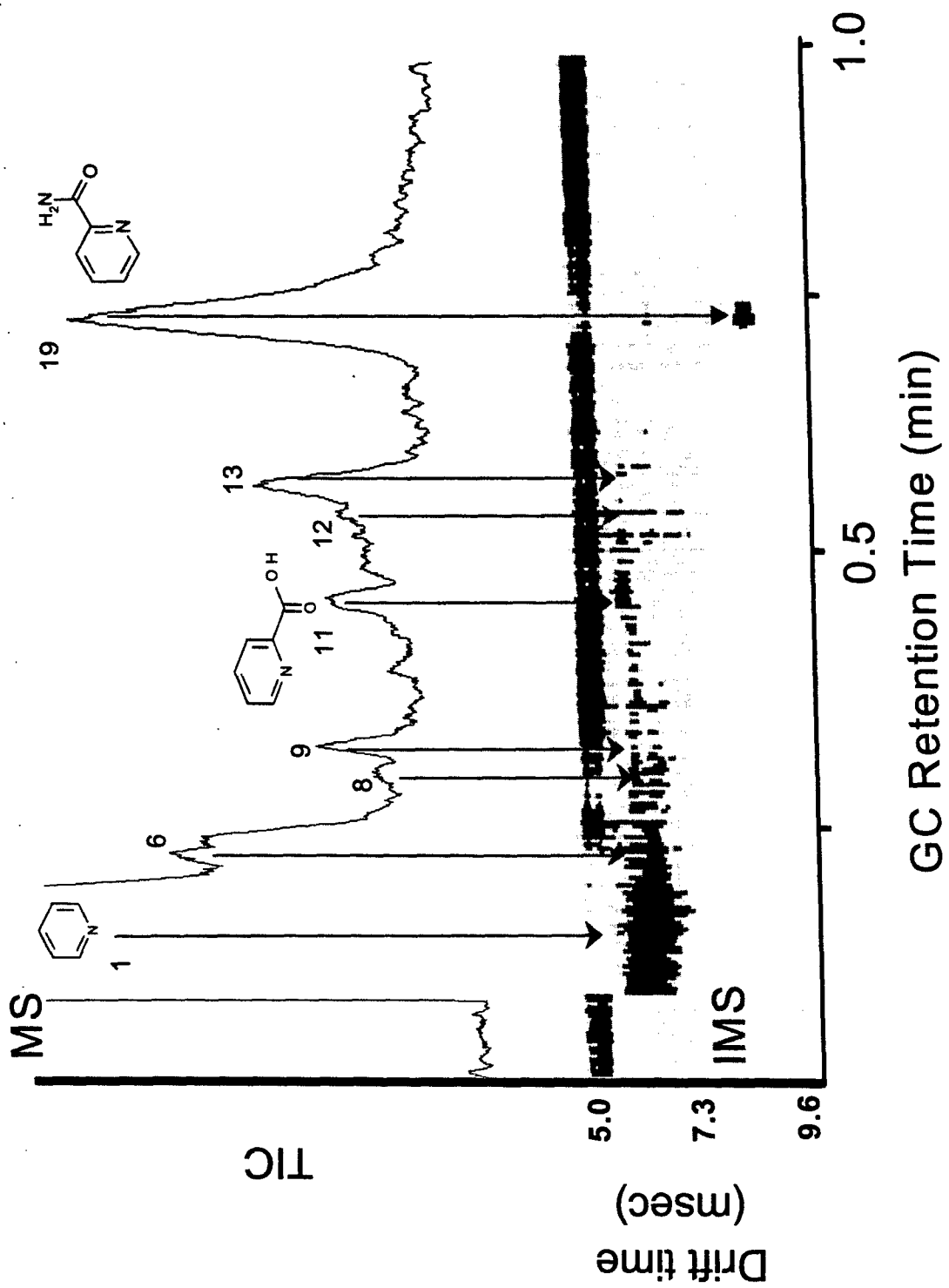


Figure 2. Py-GC-IMS and Py-GC-MS Chromatograms of Gram-positive BG Spores

The compound identities of the labeled numbers in the TIC are listed in the Table along with their structures and known bacterial origin. Most of these compounds have been identified by either the National Institute of Standards and Technology (NIST) EI mass spectral database or mass spectral comparison to commercially available authentic standards, or by both methods. For authentic standard identification, GC retention times were matched with the respective experimentally observed GC peaks. The mass spectra for compounds **16**, **17**, **21**, and **24** did not produce a satisfactory match with the NIST database because the standards were not commercially available. The taxonomic classification of the compounds was tentatively identified based on mass spectral interpretation.

Peaks **11** and **19** are particularly noteworthy because these pyrolysis products predominately originated from Gram-positive bacteria. Peak **11** is picolinic acid,²⁵ which originated from the calcium dipicolinate compound that is found only in Gram-positive spores.^{26,27} The vegetative Gram-positive organism does not contain calcium dipicolinate; therefore, the observation of picolinic acid signifies the presence of a Gram-positive spore. Peak **19** is novel³³ in that it has not been previously reported in bacterial pyrolysis publications. This compound is 2-pyridine-carboxamide and it has been shown to originate from the lysine peptide cross links in peptidoglycan.³³ The amount of the compound is high enough to form an intense dimer ion (**1**) at GC: IMS coordinates of 53 s : 8.4 ms. A weak monomer ion is observed at the same GC retention time and at a faster drift time of 6.3 ms. Why a significant amount of the substance formed and its absence from bacterial pyrolysis literature are unclear. However, pyrolysis tube airflow operational conditions are different from those in standard biological pyrolysis and Py-GC literature. Generally, a drying step is used, and a fast 20 mL/min sweep and flushing of the tube during pyrolysis facilitates the rapid removal of pyrolysis products from the heating zone. This process prevents the occurrence of secondary pyrolysis mechanisms,⁵¹ which cause degradation of the primary products to lower molecular weight fragments.

Peak **1**, a pyridine, is observed in the thermal processing of organisms in general. It originates from the protein, nucleic acid, and peptidoglycan components of microorganisms.^{25,34-37} However, peak **1** is a significant product of Gram-positive spores because it is formed predominately from the DPA chelate in calcium dipicolinate. Secondary pyrolysis mechanisms on 2-pyridinecarboxamide (**19**) can also contribute to the generation of pyridine (**1**).

Compounds **6**, **9**, **12**, and **13**, listed in the Table, are indicative of proteinaceous pyrolysis products. The appearance of protein peaks is expected because proteins constitute 50-70% of the dry weight of bacteria. However, the presence of these peaks is mostly generic with respect to bacterial biomarker utility. No direct useful bacterial distinction or discrimination information has been obtained from these substances.

The pyrolysis compounds eluted in under 0.75 min, which can be characterized as a relatively rapid analysis of a complex pyrolyzate. Except for **19**, the pyrolyzate products generally have high mobilities (low ion drift times) compared to the RIP.

3.2

Gram-positive Vegetative Cells.

The appearance of the TIC and GC-IMS dataspace of BA Δ Texas in Figure 3 are similar to that of BG in Figure 2. An intense, fast GC peak is initially observed, and it primarily consists of pyridine (1) and 2-butenoic acid or crotonic acid (4). Pyridine is found in the TICs of both bacilli (Figures 2 and 3), but crotonic acid is found only in the BA chromatogram. Pyridine can originate from the peptidoglycan cell wall layer in BA. The acid, 3-hydroxybutyric, is the monomeric subunit of the polyhydroxybutyric acid (PHBA) polymer, which is an energy storage compound in certain bacteria. Crotonic acid is the monomeric subunit pyrolysis product of PHBA. Microbiological literature shows that BG synthesizes very low amounts of PHBA,⁵² but BA produces appreciable quantities of the compound.^{36, 53}

Under pyrolysis conditions, polymer compounds usually fragment thermally into the monomeric repeat unit, compounds containing multiples and fragments of the monomer. The dimer pyrolysis product of PHBA contains two molecules of 3-hydroxybutyric acid minus a water molecule.⁵⁴ The mass spectrum of the dimer (18 in the Table) was present in Figure 3 but was not observed for BG in Figure 2. Confirmation of the presence of the dimer in BA was obtained from the same GC retention time and matching mass spectrum as that of the PHBA model compound (mass spectral data not shown).

In Figure 2, picolinic acid (11) is observed in the BG Gram-positive spore, but is absent in the Gram-positive vegetative cells of BA in Figure 3. Microbiological,^{26, 27} Py-MS,^{36, 37, 51} and, Py-GC-MS^{17, 18, 20, 25} publications provide extensive evidence that Gram-positive spores do generate picolinic acid while vegetative cells do not.

BG and BA yield an array of pyrolysis products that have their origin in the proteinaceous component (Figures 2 and 3). Because the protein component dominates the weight of dehydrated microorganisms, a significant presence of protein pyrolysis species in GC-MS bacteria analyses is typically observed. The Table outlines the most abundant species observed in Figures 2 and 3. The assignments were confirmed either by matching the GC retention time and mass spectra with standards or by matching the mass spectral with the NIST mass spectral database.

Compounds 21 and 24 were observed in the mass spectral chromatogram in Figure 3, but equivalent signals were not evident in the GC-IMS dataspace (dotted lines). These compounds were determined to be diketopiperazine (DKP) species by mass spectral interpretation. Pyrolysis has been documented to convert proteins and peptides into cyclic diamino acid products^{42, 48, 49, 55} such as compounds 21 and 24 (Table). The amino end of an amino acid residue and the carboxyl moiety of the adjacent residue cyclize by a dehydration reaction. The N atom of each residue is resident in the ring in a para position and the R groups are in the para positions as side groups on the ring. Compounds 21 and 24 were tentatively identified as the His-Val and Pro-Pro DKP species, respectively.

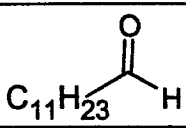
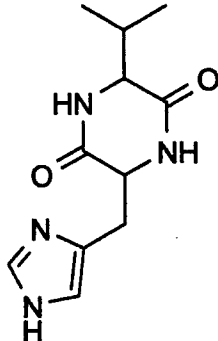
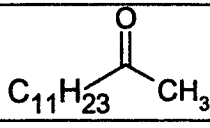
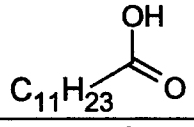
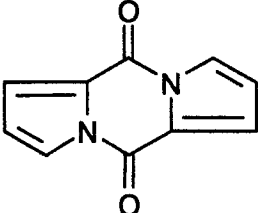
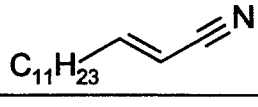
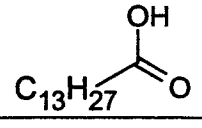
Table. GC-MS Identified Pyrolysis Products

Peak Number (N ^a , S ^b)	Structure	Name	Source	Reference
1 N, S		Pyridine	Picolinic acid, Proteins, Nucleic acids	25, 34-37
2 N, S		2-furan-carboxaldehyde, furfural	Carbohydrates	34, 38
3 N, S		5-methyl-2-furancarboxaldehyde, 5-methylfurfural	Carbohydrates	39
4 N, S		Crotonic acid	Poly (3-hydroxybutyric acid), Gram +	40
5 N, S		Benzene-acetaldehyde, benzaldehyde	Proteins	41
6 N		Hexahydropyrrolizin-3-one	Proteins	42
7 N, S		Phenol	Proteins: tyrosine	34
8 N, S		2-hydroxymethylfuran, Furfuryl alcohol	Nucleic acids, carbohydrates	43, 44
9 N, S		p-Cresol	Proteins	41, 45

Table. GC-MS Identified Pyrolysis Products (Continued)

Peak Number (N ^a , S ^b)	Structure	Name	Source	Reference
10 N, S		Phenylacetonitrile, benzonitrile	Proteins	34, 38
11 N, S		Pyridine-2-carboxylic acid, picolinic acid	Pyridine-2,5-dicarboxylic acid, Gram positive spores	26, 27
12 N		1-acetyl-1,2,3,4-tetrahydropyridine	Proteins	35
13 N		4,5,6,7-tetrahydroindole-3-one	Proteins	46
14 N		Benzene propanenitrile	Proteins	47
15 N, S		Indole	Proteins	34, 35, 41
16	(CH ₃) ₂ CH(CH ₂) ₉ CN	iso-tridecanenitrile	Branched lipids; lipoproteins	33
17	CH ₃ (CH ₂) ₁₀ CH=CH ₂	1-tridecene	Lipopolysaccharides (LPS), Gram -	33
18 N, S		Dimer of crotonic acid	Poly (3-hydroxybutyric acid), Gram +	40
19 N, S		2-pyridine-carboxamide, picolinamide	Peptidoglycan, Gram +	33

Table. GC-MS Identified Pyrolysis Products (Continued)

Peak Number (N ^a ,S ^b)	Structure	Name	Source	Reference
20 N, S	 <chem>C11H23C=O</chem>	Dodecanal	LPS, Gram -	33
21		Diketopiperazine (His-Val)	Proteins	48, 49
22 N, S	 <chem>C11H23C(=O)CH3</chem>	2-tridecanone	LPS, Gram -	33
23 N, S	 <chem>C11H23C(=O)OH</chem>	n-dodecanoic acid, lauric acid	Phospholipids, LPS, Gram -	33, 50
24		Diketopiperazine (Pro-Pro)	Proteins	48, 49
25 N	 <chem>C11H23C=C#N</chem>	2-tetradecenitrile	LPS, Gram -	33
26 N, S	 <chem>C13H27C(=O)OH</chem>	n-tetradecanoic acid, myristic acid	Phospholipids, LPS, Gram -	33, 40, 50

^aN, NIST EI-mass spectrum identification.

^bS, Standard commercially obtained compound used for identification.

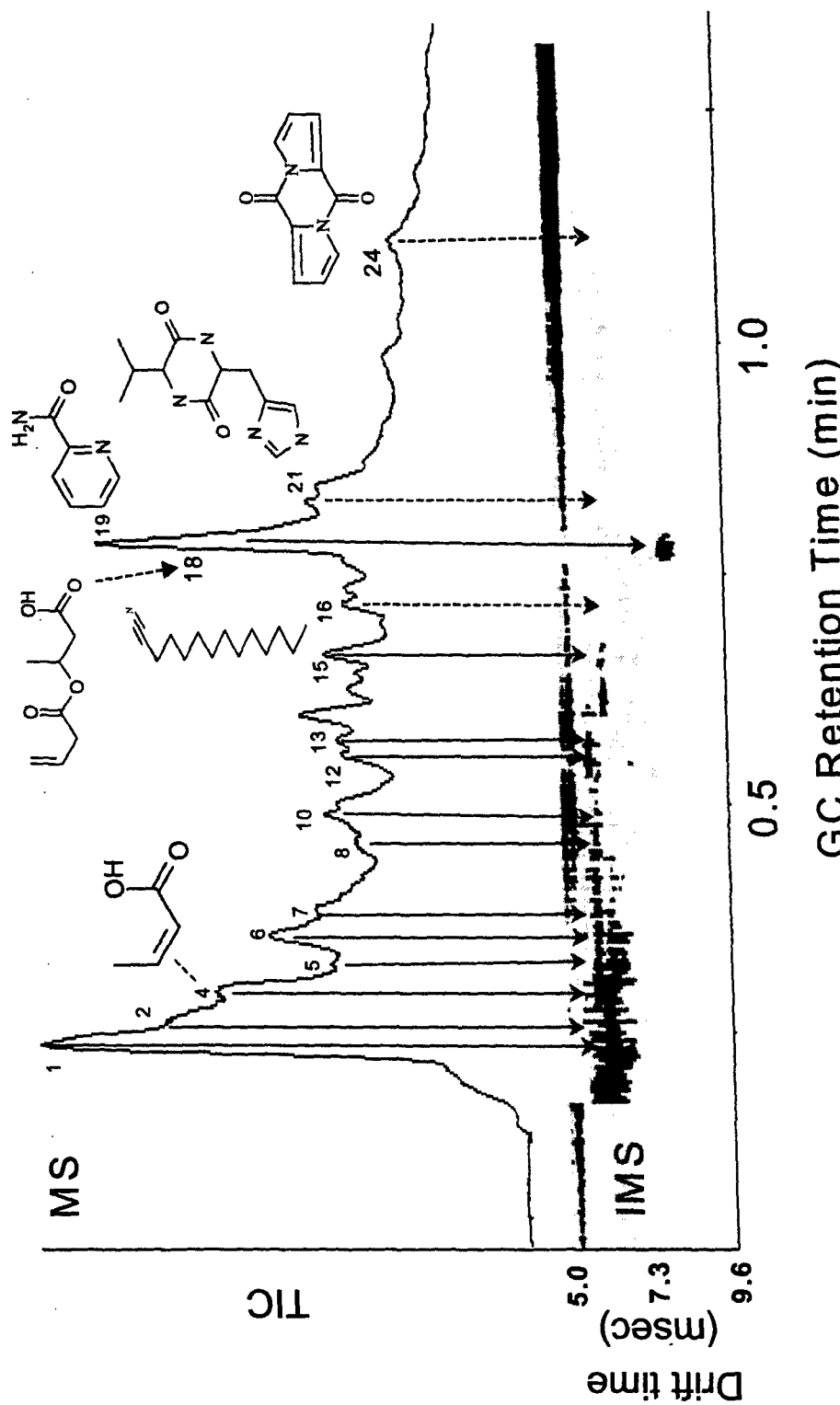


Figure 3. Py-GC-IMS and Py-GC-MS Chromatograms of the Gram-positive Δ Texas Vegetative Strain of *B. anthracis*

In addition to the DKP species, compound **16** was observed in the mass chromatogram but not in the ion mobility chromatogram. Compound **16** was tentatively identified as iso-tridecanenitrile by mass spectral interpretation. Fatty acid species in Gram-positive organisms are predominately branched⁵⁶ while those in Gram-negative organisms are linear in nature.⁵⁰ This fatty acid derivative most likely originated from intra-cellular lipoprotein species resident in the BA vegetative cells.

Compounds **16**, **21**, and **24** traversed the torturous Py-GC pathway and were registered in the mass spectrometer. However, the IMS cell was not able to respond to the compounds. Ionization is effected by the transferal of a proton in the proton-water hydrate species, formed in the 63-Ni source, to the neutral analyte only if the latter has a higher proton affinity than water. All three compounds display high proton affinity nitrogen moieties, which are amenable to proton ionization and, therefore, capable of being detected by the IMS detector. Clemmer *et al.*⁵ report the presence of small and large peptide species observed in electrospray IMS-TOF-MS proteomics studies. Woods *et al.*⁹ describe the characterization of a number of biochemical compounds, including peptides and lipids, such as sphingomyelin and cerebroside sulfate, in their matrix-assisted laser desorption-ionization (MALDI)-IMS-TOF-MS investigations.

With Gram-negative bacteria, the absence of certain pyrolyzate species in the ion mobility chromatogram is also unusual. The possible reasons for this phenomenon are outlined in the next section.

3.3 Gram-negative *E. coli*.

Figure 4 presents the Py-GC-IMS-MS mass spectra for *E. coli*. The protein pyrolysis species distribution appears very similar to that of the Gram-positive organisms (Figures 2 and 3). Except for compound **12**, all protein pyrolyzate species have the core benzene ring with an attached side chain (Table).

There are a few volatile pyrolysis species that can originate from the carbohydrate-containing biomolecules in the *E. coli* cells. These species include compounds **2**, **3**, and **8**. Pyrolysis products **4** and **18**, formed from PHBA in vegetative BA (Figure 3), were not observed in the *E. coli* mass chromatogram (Figure 4). The absence of PHBA in Figure 4 can be explained by the fact that *E. coli* does not manufacture and store PHBA^{57, 58} under normal growth conditions. A relatively small amount of 2-pyridinecarboxamide (**19**) is observed on the fast side of peak **20** as a low intensity shoulder. The amount of peptidoglycan in Gram-negative cells is about 10% of that in Gram-positive cells; therefore, compound **19** is expected to be in very low abundance.³⁰ Pyridine (**1**), which can originate from low amounts of 2-pyridinecarboxamide (**19**), is observed in the chromatogram. The amount of pyridine is relatively low when compared to the number of BG spores (Figure 2) and BA (Figure 3). Since *E. coli* does not contain calcium dipicolinate, picolinic acid (**11**) is absent in the chromatogram.

The mass chromatogram in Figure 4 is particularly rich in lipid substances. These include free fatty acids and fatty acid derivatives. Mass spectral confirmation details are presented elsewhere.³³ The outer surface layer of Gram-negative organisms such as *E. coli* is

covered with an LPS complex macromolecule. This layer produces the endotoxin material that circulates in the bloodstream when a human is infected by a Gram-negative microorganism.

The two earliest eluting fatty acid derivatives (**17, 20**) have very low intensities in the ion mobility chromatogram (vertical arrows), whereas the analogous peaks in the mass chromatogram show significant abundances. These compounds are 1-tridecene (C13, **17**) (compound **17** was determined by mass spectral interpretation), and dodecanal (C12, **20**). Compounds C12 and C13 indicate that the molecules have a backbone containing 12 and 13 carbon atoms, respectively (Table). The thermal decomposition mechanisms that lead to the appearance of these fatty acid derivatives, originating from the 3-hydroxymyristic acid portion of the LPS macromolecule, are outlined in a companion paper. The other four lipid species evident in the mass chromatogram are 2-tridecanone (C13, **22**), n-dodecanoic acid (C12) or lauric acid (**23**), 2-tetradecenenitrile (C14, **25**), and tetradecanoic acid (C14) or myristic acid (**26**). The yield of these four high boiling compounds is much lower than the two lower boiling fatty acid derivatives. Their thermal decomposition mechanisms and generation are also outlined elsewhere.³³ These relatively high boiling lipid substances are not observed in the ion mobility chromatogram from the fielded Py-GC-IMS system.

Compounds **5, 7, 10, 12, 14** and **15** indicate proteinaceous substances (Figure 4); however, compounds **17, 20, 22, 23, 25** and **26** indicate Gram-negative, LPS derived lipid substances. The latter group of compounds is an important indicator for the presence of Gram-negative organisms, which are either relatively low in intensity or just cannot be observed by the IMS detector.

3.4 Biomarker Taxonomic Utility.

Thermal processing of bacterial substances produces biochemical information that can provide more than a biological or non-biological analysis with respect to differentiation and biodetection goals and objectives. The fielded Py-GC-IMS system has shown that it can indeed produce a significant number of direct biochemical products from the thermal processing of whole, intact microorganisms. More specifically, a number of biochemical polar species, originating in cell walls that react either in a positive or negative fashion with the Gram stain, are created in the pyrolysis region; swept rapidly enough from the heated pyrolysis region and into the GC column; and eluted from the column. The Py-GC is a torturous path for polar biomolecules and has many sites for compound degradation and adsorption. Secondary thermal degradation reactions may occur in the pyrolysis source and adsorption may occur in the pyrolyzer, Py-GC interface, and GC column. The operating conditions of the pyrolysis module, however, were optimized to limit the loss of biomaterial.⁵¹ The mass chromatograms, along with authentic standards and NIST mass spectral database matching, provided confirmatory support for the biodetection potential of the system.

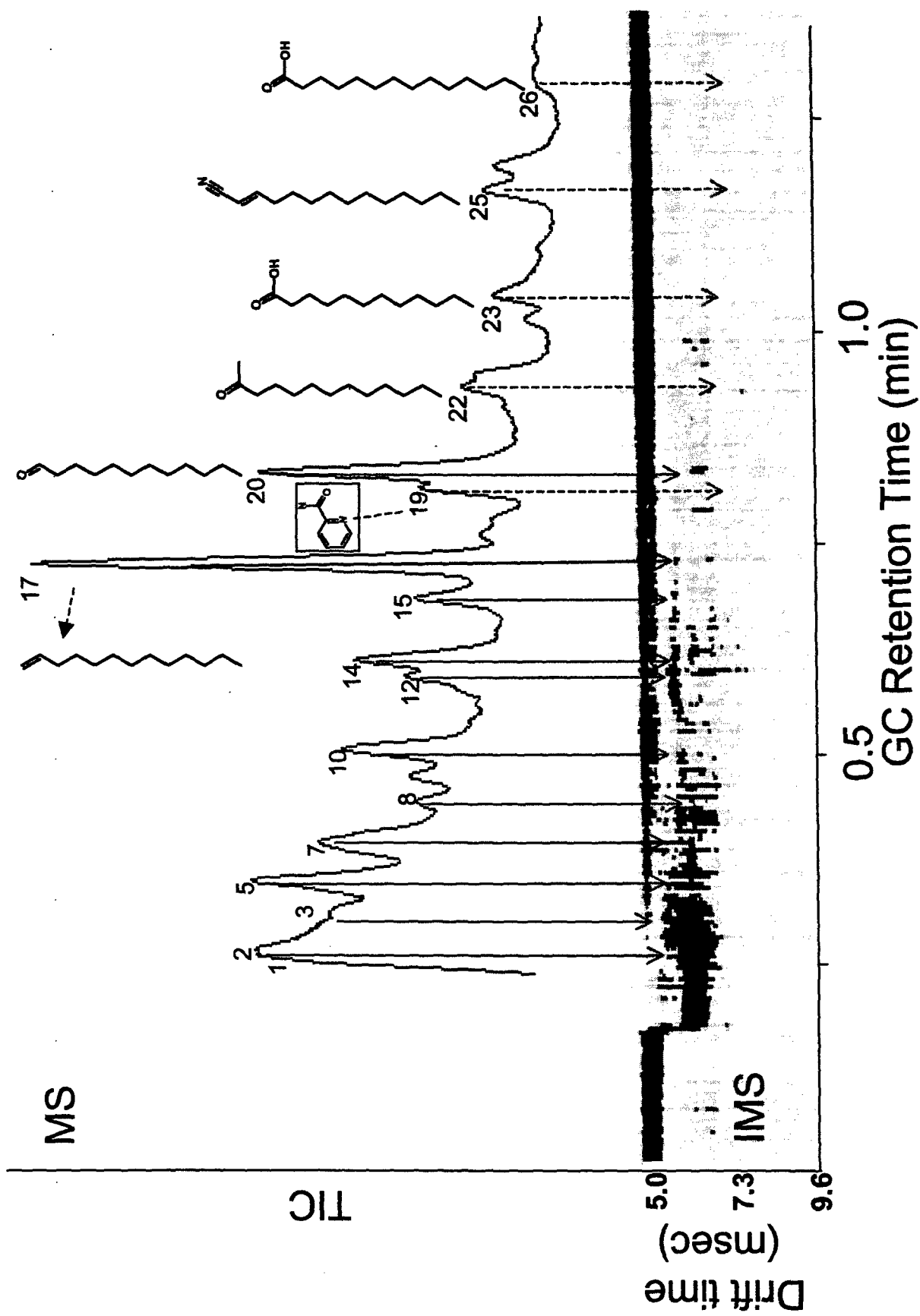


Figure 4. Py-GC-IMS and Py-GC-MS Chromatograms of Gram-negative *E. coli* K-12

The Py-GC-ambient temperature and pressure-IMS system has been shown to discriminate between a deliberately released Gram-positive BG spore, Gram-negative EH, and OV protein¹⁸⁻²⁰ aerosols between 200-800 m from the stand-alone operational system in outdoor scenarios. The present work provides mass spectral evidence of distinct biochemical compounds, produced by the pyrolysis module, from microorganisms that contain Gram-positive and Gram-negative taxonomic information. This lends credibility to the outdoor performance of the Py-GC-IMS biodetector.

3.5 Improvement of Py-GC-IMS Performance.

The Py-GC module was operated at the same conditions for the IMS and MS analyses, yet differences were observed between the two chromatograms primarily in the relatively higher temperature region of the GC column. A fundamental concern of the Py-GC-IMS system is that the temperature of the IMS detector is relatively cold and controlled to a degree by the ambient environment about the briefcase housing.¹⁸⁻²⁰ When operated in an outdoor field application, the IMS cell is subject to uneven, non-uniform temperatures: ambient environmental temperature and heat generated by internal components, including the Py-GC module, electronics, and pumping system. Good laboratory practices generally require that an analytical detector be just as hot, if not hotter, in temperature than the sample analyte introduction, processing, and transfer modules. Therefore, a constant uniform temperature about the IMS cell is warranted. A CAM IMS detector has been shown to fail irreversibly at temperatures greater than 150 °C because its internal components and solder connections are not high temperature compatible.⁶⁰ In the briefcase biodetector, a heated IMS cell can allow the observation of compounds such as **16, 21-26** as well as a greater abundance of crucial Gram-positive and Gram-negative bacterial indicator compounds such as **4, 11, 17, 19** and **20**.

The IMS detector temperature may not be the only parameter that causes minimal to negligible appearance of certain polar, biochemical compounds from the pyrolysis of microorganisms. Improvement in the signal of certain compounds may also be influenced by the pressure, sweep gas flow rate, internal gas flow patterns, and internal geometry in the IMS cell to remove excess, contaminating neutral species. For example, relatively high (atmospheric) pressure and low, ambient cell temperature can lead to condensation conditions. However, relatively lower pressures and higher temperatures can significantly reduce sample condensation on the inner surfaces of the IMS cell.

3.6 Multivariate Data Analysis.

Figure 5 shows two DF plots that provide a significant degree of differentiation for the GC-IMS dataspaces of bacterial and protein species. Even though protein species are not part of the Gram classification scheme, inclusion of this class of biological molecule in the multivariate data analyses provides more comprehensive biological discrimination capability for the Py-GC-ambient temperature and pressure-IMS system. The percent variance or information content of the dataset expressed by the first three DF vectors is DF1, 36%; DF2, 20%; and DF3, 17.9%. Both DF plots in Figure 5 show that each of the three *Bacillus* spore species is distinguishable from the other two and the vegetative *B. anthracis* strains group. The relatively low molecular weight Y and L proteins cluster as a group, while the higher molecular weight

SEB and OV species are clearly separated in multivariate DF space. The Gram-negative species also cluster as a group, while background samples are clearly separated. DF3 has the ability to distinguish the OV protein from the *B. megaterium* spore.

It appears that the differentiation and distinction of the bacterial groups in Figure 5 have a high correlation with the Gram taxonomic information from the bioanalytical results presented in Figures 2-4. The Gram-negative species cluster as a group, and the Gram-positive vegetative and spore species are clearly differentiated from each other. This find is significant because the biochemical species identified in Figures 2-4 may be able to provide distinctive characteristics concerning microbiological Gram stain taxonomy. This grouping is shown on a broader scale in Figure 5 than in Figures 2-4. The addition of protein analytes justifies the use of the Py-GC-IMS system for biological classification. Figure 5 provides a degree of credibility to the documented performance of the Py-GC-IMS biodetector at the outdoor bioaerosol field trials for the determination of bacterial and protein presence and discrimination.

4. CONCLUSIONS

The pyrolysis-gas chromatography (Py-GC) module in the fielded Py-GC ion mobility spectrometry (IMS) system generated biomolecules from bacterial species. A portion of the pyrolyzate was transferred to a mass spectrometry (MS) detector. Mass spectral analyses confirmed that these biomolecules contained microbiological discrimination information. This information appears to augment and confirm the outdoor bioaerosol performance capabilities of the briefcase Py-GC-IMS because taxonomically useful pyrolyzate species were generated and detected by the biodetector. The 2-pyridinecarboxamide and 3-hydroxymyristic acid derivative biomolecules can be used as biomarker indicators for certain classes of bacteria. These biomolecules contain microbiological taxonomic information. The biomarkers, both individually and collectively, correlate to a significant degree with the microbiological Gram stain classification scheme. The acid, a 2-pyridinecarboxamide, produced by the fielded Py-GC-IMS, can be directly correlated to Gram-positive classification information, and the 3-hydroxymyristic acid derivative compounds can be directly correlated to Gram-negative bacteria. An added benefit is that these specific biomarkers are invariant to microbiological growth and culture parameters such as growth media conditions, age of the cells, growth temperatures, and harvest conditions. Observation of these biomarkers can confirm the presence of either Gram-positive or Gram-negative microorganisms. Picolinic acid and polyhydroxybutyric acid (PHBA) pyrolyzate species are not directly related to the Gram stain phenomenon. However, they correlate with a Gram-positive or Gram-negative organism and are added benefits to the information content in a Py-GC-IMS spectrum.

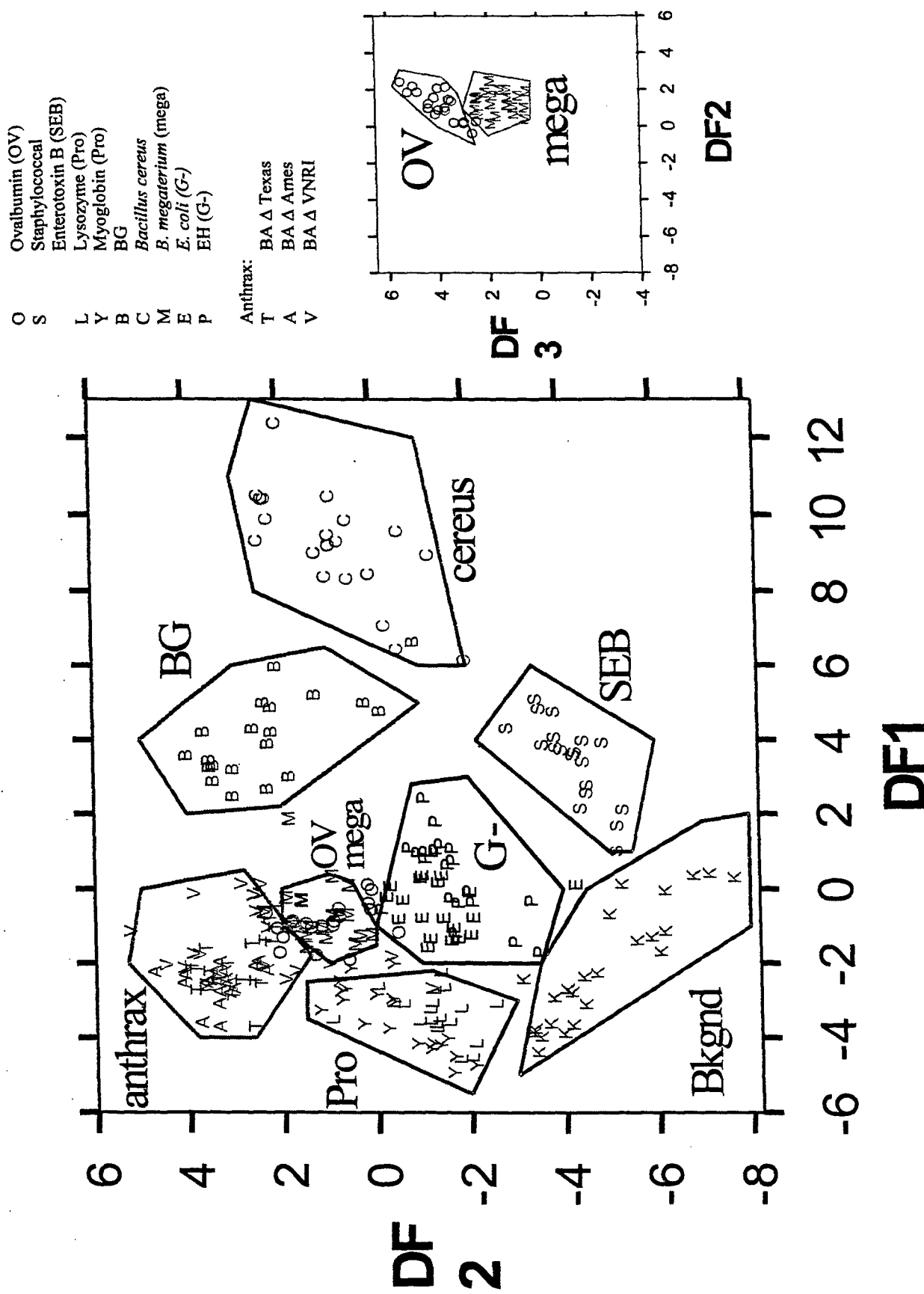


Figure 5. DF Plots of the Analysis of Liquid Suspensions of Gram-positive, Gram-negative, and Protein Biological Species

Specific instrumental parameter modifications were suggested to improve the detection of taxonomically useful information, such as applying a relatively high isothermal temperature to the analytically challenged ambient temperature and pressure IMS cell. Certain relatively high boiling lipid and diketopiperazine (DKP) polar compounds, observed in the mass chromatogram, are of very low intensity or absent in the corresponding ion mobility chromatogram. Together, the mass spectral information generated and transferred from the Py-GC module, the discriminant factor (DF) analyses of the GC-IMS dataspaces of a suite of biological samples and the documented performance of the fielded Py-GC-IMS system provide microbiological, scientific, technical and operational support for the utility of the system in biological classification and discrimination scenarios.

Blank

LITERATURE CITED

1. Eiceman, G.A.; Karpas, Z., Eds. *Ion Mobility Spectrometry*; CRC Press: Boca Raton, FL, 1994.
2. Turner, R.B. Transitioning Analytical Instrumentation from the Laboratory to Harsh Environments. *Pure Appl. Chem.* **2002**, *74*, pp 2317-2322.
3. Hoaglund-Hyzer, C.S.; Clemmer, D.E. Ion Trap/Ion Mobility/Quadrupole/Time-of-Flight Mass Spectrometry for Peptide Mixture Analysis. *Anal. Chem.* **2001**, *73*, pp 177-184.
4. Barnes, C.A.S.; Hilderbrand, A.E.; Valentine, S.J.; Clemmer, D.E. Resolving Isometric Peptide Mixtures: A Combined HPLC/Ion Mobility-TOFMS Analysis of a 4000-Component Combinatorial Library. *Anal. Chem.* **2002**, *74*, pp 26-36.
5. Myung, S.; Lee, Y.J.; Moon, M.H.; Taraszka, J.; Sowell, R.; Koeniger, S.; Hilderbrand, A.E.; Valentine, S.J.; Cherbas, L.; Cherbas, P.; Kaufmann, T.C.; Miller, D.F.; Mechref, Y.; Novotny, M.; Ewing, M.A.; Sporleder, C.R.; Clemmer, D.E. Development of High-Sensitivity Ion Trap Ion Mobility Spectrometry Time-of-Flight Techniques: A High Throughput Nano-LC-IMS-TOF Separation of Peptides Arising from a *Drosophila* Protein Extract. *Anal. Chem.* **2003**, *75*, pp 5137-5145.
6. Gillig, K.J.; Ruotolo, B.; Stone, E.G.; Russell, D.R.; Fuhrer, K.; Gonin, M.; Schultz, A.J. Anal. Coupling High Pressure MALDI with Ion Mobility/Orthogonal Time-of-Flight Mass Spectrometry. *Anal. Chem.* **2000**, *72*, pp 3965-3971.
7. Woods, A.S.; Koomen, J.M.; Ruotolo, B.T.; Gillig, K.J.; Fuhrer, K.; Gonin, M.; Egan, T.F.; Schultz, J.A. A Study of Peptide-Peptide Interactions using MALDI Ion Mobility o-TOF and ESI Mass Spectrometry. *J. Am. Soc. Mass Spectrom.* **2002**, *13*, pp 166-169.
8. McLean, J.A.; Russell, D.H. Sub-femtomole Peptide Detection in Ion Mobility-Time-of-Flight Mass Spectrometry Measurements. *J. Proteome Res.* **2003**, *2*, pp 427-430.
9. Woods, A.S.; Ugarov, M.; Egan, T.; Koomen, J.; Gillig, K.J.; Fuhrer, K.; Gonin, M.; Schultz, J.A. Lipid/Peptide/Nucleotide Separation with MALDI-Ion Mobility-TOF MS. *Anal. Chem.* **2004**, *76*, pp 2187-2195.
10. Matz, L.M.; Asbury, G.R.; Hill, Jr., H.H. Two-Dimensional Separation with Electrospray Ionization Ambient Pressure High-Resolution Ion Mobility Spectrometry/Quadrupole Mass Spectrometry. *Rapid Commun. Mass Spectrom.* **2002**, *16*, pp 670-675.

11. Matz, L.M.; Steiner, W.E.; Clowers, B.H.; Hill, H.H., Jr. Evaluation of Micro-Electrospray Ionization with Ion Mobility Spectrometry/Mass Spectrometry. *Intl. J. Mass Spectrom.* **2002**, *213*, pp 191-202.
12. Steiner, W.E.; Clowers, B.H.; English, W.A.; Hill, H.H., Jr. Atmospheric Pressure Matrix-Assisted laser Desorption/Ionization with Analysis by Ion Mobility Time-of-Flight Mass Spectrometry. *Rapid Commun. Mass Spectrom.* **2004**, *18*, pp 1-7.
13. Lee, S; Gotts, N.G.; von Helden, G.; Bowers, M.T. Evidence from Ion Chromatography Experiments that Met-Cars are Hollow Cage Clusters. *Sci.*, **1995**, *267*, pp 999-1001.
14. Bowers, M.T.; Kemper, P.R.; von Helden, G.; van Koppen, P.A.M. Gas-Phase Ion Chromatography: Transition Metal State Selection and Carbon Cluster Formation. *Sci.*, **1993**, *260*, pp 1446-1451.
15. Dugourd, Ph.; Hudgins, R.R.; Clemmer, D.E.; Jarrold, M.F. High-Resolution Ion Mobility Measurements. *Rev. Sci. Instrumen.* **1997**, *68*, pp 1122-1129.
16. Fye, J.L.; Jarrold, M.F. Ion Mobility Studies of Metal-Coated Fullerenes. *Intl. J. Mass Spectrom.* **1999**, *185/186/187*, pp 507-515.
17. Dworzanski, J.P.; McClenen, W.H.; Cole, P.A.; Thornton, S.N.; Meuzelaar, H.L.C.; Arnold, N.S.; Snyder, A.P. Field-Portable, Automated Pyrolysis-GC/IMS System for Rapid Biomarker Detection in Aerosols: A Feasibility Study. *Field Anal. Chem. Technol.* **1997**, *1*, pp 295-305.
18. Snyder, A.P.; Maswadeh, M.M.; Parsons, J.A.; Tripathi, A.; Meuzelaar, H.L.C.; Dworzanski, J.P.; Kim, M.-G. Field Detection of Bacillus Spore Aerosols with Stand-Alone Pyrolysis-Gas Chromatography-Ion Mobility Spectrum. *Field Anal. Chem. Technol.* **1999**, *3*, pp 315-326.
19. Snyder, A.P.; Maswadeh, M.M.; Tripathi, A.; Dworzanski, J.P. Detection of Gram-Negative *Erwinia* herbicola Outdoor Aerosols with Pyrolysis-Gas Chromatography/Ion Mobility Spectrometry. *Field Anal. Chem. Technol.* **2000**, *4*, pp 111-126.
20. Snyder, A.P.; Tripathi, A.; Maswadeh, M.M.; Ho, J.; Spence, M. Field Detection and Identification of a Bioaerosol Suite by Pyrolysis-Gas Chromatography-Ion Mobility Spectrometry. *Field Anal. Chem. Technol.* **2001**, *5*, pp 190-204.
21. Snyder, A.P.; Maswadeh, M.M.; Tripathi, A.; Eversole, J.; Ho, J.; Spence, M. Orthogonal Analysis of Mass and Spectral Based Technologies for the Field Detection of Bioaerosols. *Anal. Chim. Acta* **2004**, *513*, pp 365-377.

22. Eiceman, G.A. Advances in Ion Mobility Spectrometry: 1980-1990. *Crit. Rev. Anal. Chem.* **1991**, 22, pp 471-490.

23. Baumbach, J.I.; Eiceman, G.A. Ion Mobility Spectrometry; Arriving on Site and Moving Beyond a Low Profile. *Appl. Spectro.* **1999**, 53, pp 338A-355A.

24. Vinopal, R.T.; Jadamec, J.R.; deFur, P.; Demars, A.L.; Jakubielski, S.; Green, C.; Anderson, C.P.; Dugas, J.E.; DeBono, R.F. Fingerprinting Bacterial Strains Using Ion Mobility Spectrometry. *Anal. Chim. Acta* **2002**, 457, pp 83-95.

25. Snyder, A.P.; Thornton, S.N.; Dworzanski, J.P.; Meuzelaar, H.L.C. Detection of the Picolinic Acid Biomarker in *Bacillus* Spores Using a Potentially Field-Portable Pyrolysis-Gas Chromatography-Ion Mobility Spectrometry System. *Field Anal. Chem. Technol.* **1996**, 1, pp 49-58.

26. Breed, R.S.; Murray, E.G.D.; Smith, N.R., Eds. *Bergey's Manual of Determinative Bacteriology*; 7th ed. The Williams & Wilkins Company: Baltimore, 1957, pp 295-305.

27. Gould, G.W.; Hurst, A., Eds. *The Bacterial Spore*; Academic Press: New York, NY, 1969.

28. Snyder, A.P.; Harden, C.S.; Brittain, A.H.; Kim, M.-G.; Arnold, N.S.; Meuzelaar, H.L.C. Portable Hand-Held Gas Chromatography/Ion Mobility Spectrometry Device. *Anal. Chem.* **1993**, 65, pp 299-306.

29. Snyder, A.P.; Maswadeh, W.M.; Tripathi, A. ECBC, Edgewood, MD. Jan-Feb, 2001.

30. Lennette, E.H.; Balows, A.; Hausler, W.J., Jr.; Eds. *Manual of Clinical Microbiology*; Chapter 98; American Society for Microbiology: Washington, DC, 1980.

31. Kroonenberg, P.M., Ed. *Three-Mode Principal Component Analysis: Theory and Applications*; DWO Press: Leiden, The Netherlands, 1983.

32. Marengo, E.; Leardi, R.; Robotti, E.; Righetti, P.G.; Antonucci, F.; Cecconi, D. Application of Three-Way Principal Component Analysis to the Evaluation of Two-Dimensional Maps in Proteomics. *J. Proteome Res.* **2003**, 2, pp 351-360.

33. Hair, J.F., Jr.; Anderson, R.E.; Tatham, R.L.; Black, W.C. *Multivariate Data Analysis*; Prentice-Hall, Inc.: Upper Saddle River, NJ, 1998.

34. Dworzanski, J.P.; Tripathi, A.; Snyder, A.P.; Maswadeh, M.M.; Wick, C.H. Novel Biomarkers for Gram-Type Differentiation of Bacteria by Pyrolysis-Gas Chromatography-Mass Spectrometry. *J. Anal. Appl. Pyrolysis* **2005**, 73, pp 29-38.

35. Fox, A.; Morgan, S.L. The Chemotaxonomic Characterization of Microorganisms by Capillary Gas Chromatography and Gas Chromatography-Mass Spectrometry. In *Rapid Detection and Identification of Microorganisms*: Chapter 5; Nelson, W.H., Ed.; VCH Publishers: Deerfield Beach, FL, 1985, pp 135-164.

36. Stankiewicz, B.A.; van Bergen, P.F.; Duncan, I.J.; Carter, J.F.; Briggs, D.E.G.; Evershed, R.P. Recognition of Chitin and Proteins in Invertebrate Cuticles Using Analytical Pyrolysis/Gas Chromatography and Pyrolysis/Gas Chromatography/Mass Spectrometry. *Rapid Commun. Mass Spectrom.* **1996**, *10*, pp 1747-1757.

37. Beverly, M.B.; Voorhees, K.J.; Hadfield, T.L. Direct Mass Spectrometric Analysis of *Bacillus* Spores. *Rapid Commun. Mass Spectrom.* **1999**, *13*, pp 2320-2326.

38. Beverly, M.B.; Basile, F.; Voorhees, K.J.; Hadfield, T.L. A Rapid Approach for the Detection of Dipicolinic Acid in Bacterial Spores using Pyrolysis/Mass Spectrometry. *Rapid Commun. Mass Spectrom.* **1996**, *10*, pp 455-458.

39. Eudy, L.W.; Walla, M.D.; Morgan, S.L., Fox, A. Gas Chromatographic-Mass Spectrometric Determination of Muramic Acid Content and Pyrolysis Profiles for a Group of Gram-positive and Gram-negative Bacteria. *Analyst* **1985**, *110*, pp 381-385.

40. Medley, E.E.; Simmonds, P.G.; Manatt, S.L. A Pyrolysis Gas Chromatography Mass Spectrometry Study of the Actinomycete *Streptomyces longisporosflavus*. *Biomed. Mass Spectrom.* **1975**, *2*, pp 261-265.

41. Grassie, N.; Murray, E.J.; Holmes, P.A. The Thermal Degradation of Poly(-D-beta-hydroxybutyric acid): Part 3-The Reaction Mechanism. *Polymer Degradation Stability* **1984**, *6*, pp 127-134.

42. Chiavari, G.; Galletti, G. Pyrolysis-Gas Chromatography/Mass Spectrometry of Amino Acids. *J. Anal. Appl. Pyrolysis* **1992**, *24*, pp 123-137.

43. Smith, G.G.; Reddy, G.S.; Boon, J.J. Gas Chromatographic-Mass Spectrometric Analysis of the Curie-Point Pyrolysis Products of Some Dipeptides and Their Diketopiperazine. *J. Chem. Soc. Perkin Trans.* **1988**, *II*, pp 203-211.

44. Schrodter, R.; Baltes, W. Pyrolysis of Various Furan Model Compounds. *J. Anal. Appl. Pyrolysis* **1991**, *19*, pp 131-137.

45. van der Kaaden, A.; Haverkamp, J.; Boon, J.J.; de Leeuw, J.W. Analytical Pyrolysis of Carbohydrates. 1. Chemical Interpretation of Matrix Influences on Pyrolysis-Mass Spectra of Amylose Using Pyrolysis-gas Chromatography-Mass Spectrometry. *J. Anal. Appl. Pyrolysis* **1983**, *5*, pp 199-220.

46. Tsuge, S.; Matsubara, H. High-Resolution Pyrolysis-Gas Chromatography of Proteins and Related Materials. *J. Anal. Appl. Pyrolysis* **1985**, *8*, pp 49-64.

47. Boon, J.J.; de Leeuw, J.W. Amino Acid Sequence Information in Proteins and Complex Proteinaceous Material Revealed by Pyrolysis-Capillary Gas Chromatography-Low and High Resolution Mass Spectrometry. *J. Anal. Appl. Pyrolysis* **1987**, *11*, pp 313-327.

48. Voorhees, K.J.; Zhang, W.; Hendricker, A.D.; Murugaverl, B. An Investigation of the Pyrolysis of Oligopeptides by Curie-Point Pyrolysis-Tandem Mass Spectrometry. *J. Anal. Appl. Pyrolysis* **1994**, *30*, pp 1-16.

49. Hendricker, A.D.; Voorhees, K.J. Amino Acid and Oligopeptide Analysis Using Curie-Point Pyrolysis Mass Spectrometry with In-Situ Thermal Hydrolysis and Methylation: Mechanistic Considerations. *J. Anal. Appl. Pyrolysis* **1998**, *48*, pp 17-33.

50. Hendricker, A.D.; Voorhees, K.J. An Investigation into the Curie-Point Pyrolysis-Mass Spectrometry of Glycyl Dipeptides. *J. Anal. Appl. Pyrolysis* **1996**, *36*, pp 51-70.

51. Wilkinson, S.G. In *Microbial Lipids*; Chapter 7; Ratledge, C.; Wilkinson, S.G., Eds.; Academic Press: London, UK, 1988.

52. Tripathi, A.; Maswadeh, M.M.; Snyder, A.P. Optimization of Quartz Tube Pyrolysis Atmospheric Pressure Ionization Mass Spectrometry for the Generation of Bacterial Biomarkers. *Rapid Commun. Mass Spectrom.* **2001**, *15*, pp 1672-1680.

53. Reusch, R.A.; Sadoff, H.L. D-(-)-Poly-Beta-Hydroxybutyrate in Membranes of Genetically Competent Bacteria. *J. Bacteriol.* **1983**, *156*, pp 778-788.

54. Watt, B.E.; Morgan, S.L.; Fox, A. 2-Butenoic Acid, a Chemical Marker for Poly-Beta-Hydroxybutyrate Identified by Pyrolysis-Gas Chromatography/Mass Spectrometry in Analyses of Whole Microbial Cells. *J. Anal. Appl. Pyrolysis* **1991**, *19*, pp 237-249.

55. Morikawa, H.; Marchessault, R.H. Pyrolysis of Bacterial Polyalkanoates. *Can. J. Chem.* **1981**, *59*, pp 2306-2313.

56. Noguerola, A.S.; Murugaverl, B.; Voorhees, K.J. An Investigation of Dipeptides Containing Polar and Nonpolar Side Groups by Curie-Point Pyrolysis Tandem Mass Spectrometry. *J. Am. Soc. Mass Spectrom.* **1992**, *3*, pp 750-756.

57. O'Leary, W.M.; Wilkinson, S.G. In *Microbial Lipids*; Chapter 5; Ratledge, C.; Wilkinson, S.G., Eds.; Academic Press: London, UK, 1988.

58. Reusch, R.; Hiske, T.; Sadoff, H.; Harris, R.; Beveridge, T. Cellular Incorporation of Poly-Beta-Hydroxybutyrate into Plasma Membranes of *Escherichia coli* and *Azotobacter vinelandii* Alters Native Membrane Structure. *Can. J. Microbiol.* 1987, 33, pp 435-444.

59. Reddy, C.S.K.; Ghai, R.; Rashmi, V.C.K. Polyhydroxyalkanoates: An Overview. *Bioresource Technol.* 2003, 87, pp 137-146.

60. Arnold, N.A., University of Utah, Salt Lake City, UT, 2004